Archives of Orthopaedic and Trauma Surgery (2019) 139:751–760
https://doi.org/10.1007/s00402-018-03106-2

ORTHOPAEDIC SURGERY

Design and preliminary biomechanical analysis of a novel motion preservation device for lumbar spinal disease after vertebral corpectomy

Jiantao Liu[1] · Xijing He[2] · Zhengchao Gao[2] · Binbin Niu[2] · Dongbo Lv[1] · Yanzheng Gao[1]

Received: 12 September 2018 / Published online: 12 February 2019

Abstract

Objective To design a novel prosthesis, a movable artificial lumbar complex (MALC), for non-fusion reconstruction after lumbar subtotal corpectomy and to evaluate the stability, range of motion and load-bearing strength in the human cadaveric lumbar spine.

Methods Biomechanical tests were performed on lumbar spine specimens from 15 healthy cadavers which were divided in three groups: non-fusion, fusion and intact group. The range of motion (ROM), stability and load-bearing strength were measured.

Results The prosthesis was composed of three parts: the upper and lower artificial lumbar discs and the middle artificial vertebra. Both the MALC and titanium mesh cage re-established vertebral height, and no spinal cord compression or prosthesis dislocation was observed at the operative level. Regarding stability, there was no significant difference in all directions between the intact group and non-fusion group ($P > 0.05$). Segment movements of the specimens in the non-fusion group revealed significantly decreased T12–L1 ROM and significantly increased L1–2 and L2–3 ROM in flexion/extension and lateral bending compared with those in the fusion group ($P < 0.05$). Regarding load-bearing strength, when the lumbar vertebra was ruptured, there was no damage to the MALC and titanium mesh cage, but the maximum load in the non-fusion group was larger ($P > 0.05$).

Conclusions Compared with titanium cages, the MALC prosthesis not only restored the vertebral height and effectively preserved segment movements without any abnormal gain of mobility in adjacent inter-vertebral spaces but also bore the lumbar load and reduced the local stress load of adjacent vertebral endplates.

Keywords Spine · Prostheses and implants · Biomechanical phenomena · Non-fusion · Artificial vertebral body

Introduction

Trauma, tumors, and autoimmune diseases of the lumbar spine can affect patients' function, quality of life and prognosis [1, 2]. Vertebral body corpectomy followed by interbody fusion has become a common treatment for these diseases [3–6]. Although the effect of spinal cord decompression, replacement of vertebral body and reconstruction of spinal stability has been notable [7], loss of mobility in the fused region of the spine is an insurmountable hurdle [8] that affects the quality of life for patients to some extent. Additionally, many studies have confirmed loss of mobility in the fused region as a fundamental cause of the acceleration of degeneration in adjacent inter-vertebral discs [9, 10]. Although artificial inter-vertebral discs, artificial medullary nuclei and posterior dynamic internal fixation systems have been widely used clinically and have been somewhat successful in preserving the activity of the operative area [11–14], they cannot be used due to their own structural limitations when lumbar corpectomy must be performed for the treatment of diseases, such as tumors, and fractures. Therefore, to avoid the degeneration of adjacent segments and the decrease of quality of life caused by the loss of mobility of

✉ Yanzheng Gao
doctorgao63@163.com

[1] Department of Spine and Spinal Cord, Henan Provincial People's Hospital, No.7, the Weft Fifth Road, Jinshui District, Zhengzhou, Henan, People's Republic of China

[2] Department of Orthopedics, Second Affiliated Hospital of Xi'an Jiaotong University, Xi'an, Shaanxi, People's Republic of China

the operative site after vertebral resection and fusion, it is of great clinical significance to develop a new prosthesis that can not only reconstruct the height and stability of the vertebral body, but also retain a certain mobility just like the artificial intervertebral disc. We designed a moveable artificial lumbar complex (MALC) prosthesis as a solution, and we previously studied the in vitro biomechanics of goats and got good results [15]. In this study, we are aimed to assess its biomechanical properties in fresh human cadavers.

Methods and materials

Ethics statement

This study was strictly performed in accordance with the Code of Ethics of the World Medical Association (Declaration of Helsinki) and approved by the Ethics Committee of Xian Jiaotong University (Number: 2017-765). All the specimens were obtained via informed donation from cadaveric materials, in accordance with federal and state regulations.

Specimens

A total of fifteen human lumbar spine specimens (T_{12}–L_5; average donor age: 46.4±7.0 years; 8 male, 7 female) were provided by the Anatomy and Pathology Department of the Medical College of Xi'an Jiaotong University at no cost. X-ray (QDR-2000, Hologic, Waltham, MA) images (Fig. 1a, b) were obtained to confirm the absence of skeletal abnormalities. BMD (MEDIX90, French Mr Stowe, France) were obtained to ensure that none of the specimens had osteoporosis. All the specimens were randomly divided into three groups: the intact group, fusion group and non-fusion group, and the muscle and peripheral soft tissues were removed with caution, with the ligament and capsule of the facet joint kept intact. Then, all the specimens were double-wrapped in plastic bags and preserved in a freezer at a temperature of minus 20 °C before the experiment.

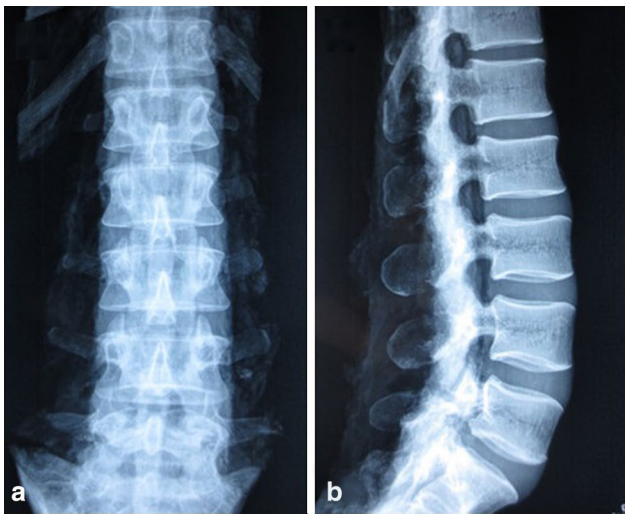

Fig. 1 X-ray images of human specimens. *a* anterior–posterior X-ray image, *b* lateral X-ray image

Design of the MALC

In our previous study [16], we collected anatomical data from whole lumbar spines from 60 healthy volunteers by Mimics (Version 16.0, Interactive Medical Image Control System, Materialize Company, Belgium). According to these anatomical data, we designed the MALC prosthesis (China Invention Patent Number: ZL201610285603.X) with Solidworks (Version 2013, Dassault Systems S.A, USA) computer-aided software. The prosthesis (Fig. 2a–c) consists of one middle artificial vertebra (Fig. 2d) and two artificial discs (Fig. 2e). The artificial vertebra was shaped like a half-cylinder with the depression in the posterior surface to protect the spinal cord. The lateral surface of the artificial vertebra is equipped with through slots and some randomly distributed circular grooves for bone implantation and fusion with residual bone. Both the upper and lower surfaces of the vertebral implant are equipped with annular grooves, and half of the sphere (Fig. 2f) located inside the groove is composed of the ball-and-socket joint along with the spherical shell structure of the artificial disc. The artificial disc is composed of the base, cylindrical projection and the curved wing, which has two screw holes that are not in the same horizontal plane. The curved wing was on the lateral side of the base with an angle of approximately 85° between them. At the end of the cylindrical projection, there was a spherical shell structure with two curved convex spherical shells in its margins, which plays an important role in preventing the dislocation of the ball-and-socket joint. To reduce friction, the ball-and-socket joint was polished. The assembly process of the prosthesis was as follows. First, the sphere was assembled on the artificial vertebral body, and the curved convex of the spherical shell of the artificial disc was then aligned with the gap of the annular groove. The spherical shell was then placed into the groove and served as the ball-and-socket joint within the sphere. Finally, the artificial disc was rotated 90° so that it could not be displaced from the annular groove. The metal part of the MALC prosthesis (Fig. 3), composed of Ti6Al4V alloy, was produced by three-dimensional (3D) metal printing technology (Bright Laser Rapid Prototyping, Technology Co., Ltd., Xi'an, China), and the sphere, composed of polyethylene, was processed using a high-precision numerical control machine (Beijing Chunlizhengda Medical Instruments, Co., Ltd., Beijing, China). Theoretically, the prosthesis not only replaced the excised vertebrae and discs but also preserved the ROM of the disc, which was 5° in

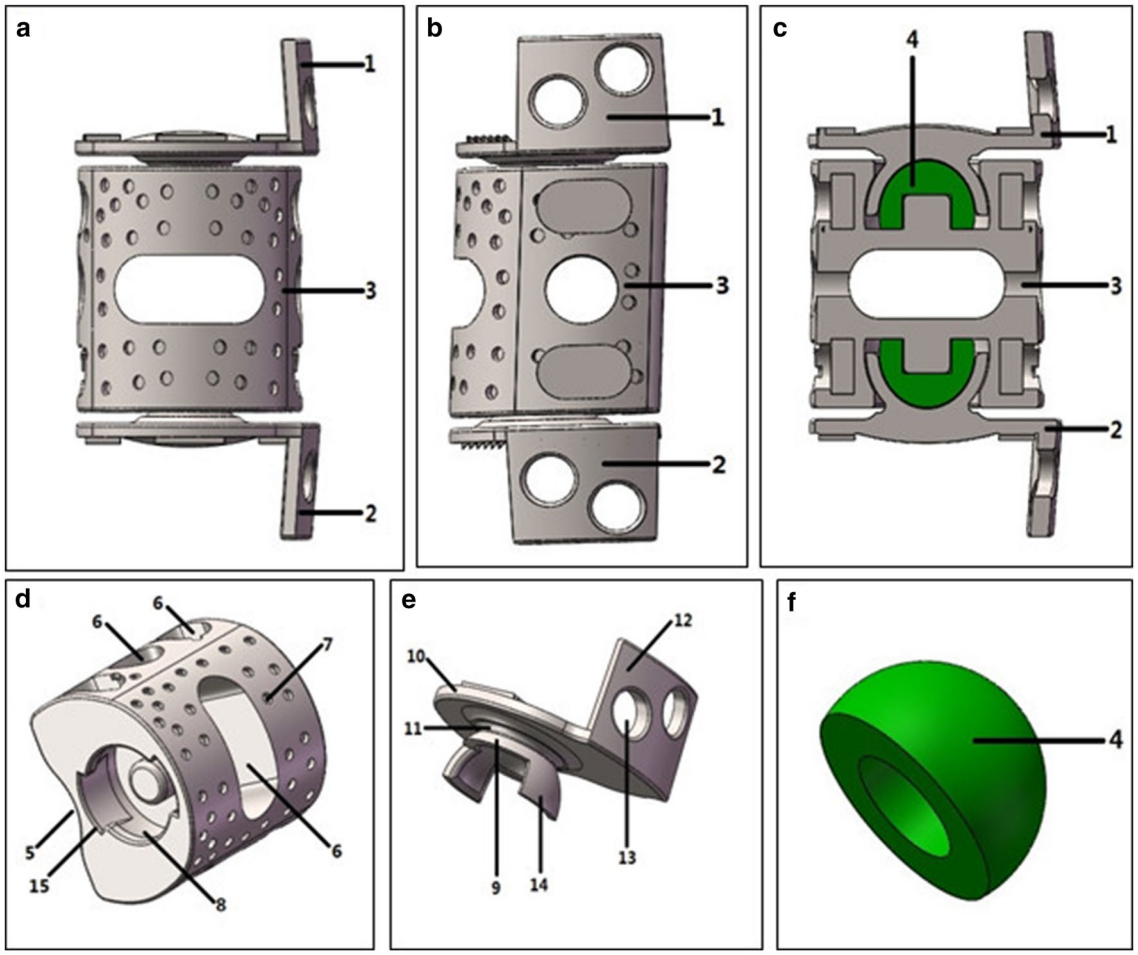

Fig. 2 Three-dimensional diagrams of the MALC prosthesis. **a** Front view of the MALC prosthesis; **b** lateral view of the MALC prosthesis; **c** profile view of the MALC prosthesis; **d** oblique view of the artificial vertebrae; **e** oblique view of the artificial disc; and **f** oblique view of the half sphere located inside the groove. 1, 2. The upper and lower artificial discs; 3. The artificial vertebrae; 4. The half sphere located inside the groove; 5. The depression in the posterior surface of the artificial vertebrae; 6. Through slots; 7. Some randomly distributed circular grooves; 8. The annular groove; 9. The spherical shell; 10. The base; 11. The cylindrical projection; 12. The curved wing; 13. Two screw holes; 14. The curved convex spherical shells; 15. The gap of the annular groove

flexion, extension, and lateral bending and 360° in axial rotation. Additionally, the size of the artificial vertebra and ROM of the artificial discs in flexion, extension, and lateral bending can be adjusted according to the anatomical parameters.

Model building

An experienced orthopedic surgeon performed a lumbar corpectomy for all specimens in the fusion and non-fusion groups at the L2 level. A major incision of the L2 vertebra was made using a bone rongeur for decompression. The L1–2 and L2–3 discs were removed using a pituitary rongeur. In the non-fusion group, the MALC prosthesis was assembled and then implanted at the L2 level, followed by screw fixation at L1 and L3. In the fusion group, a 3D printed titanium mesh cage designed by our team [17] combined with a titanium plate was implanted at the same level, followed by screw fixation. Then, anterior–posterior and lateral X-ray imaging, as well as CT scanning and three-dimensional reconstruction with a slice thickness of 0.5 mm were performed to inspect the position of the implants and spinal cord status.

Biomechanical tests

MTS 858 Mini Bionix II biomaterial testing system (MTS, USA) was used for the biomechanical tests in the State Key Laboratory of Mechanical Strength and Vibration of Xi'an Jiaotong University. According to the testing criteria for spinal implants published by Wilke and co-workers [18], the T12–L3 segments of the lumbar specimens were embedded in a special metal mold containing polymethylmethacrylate

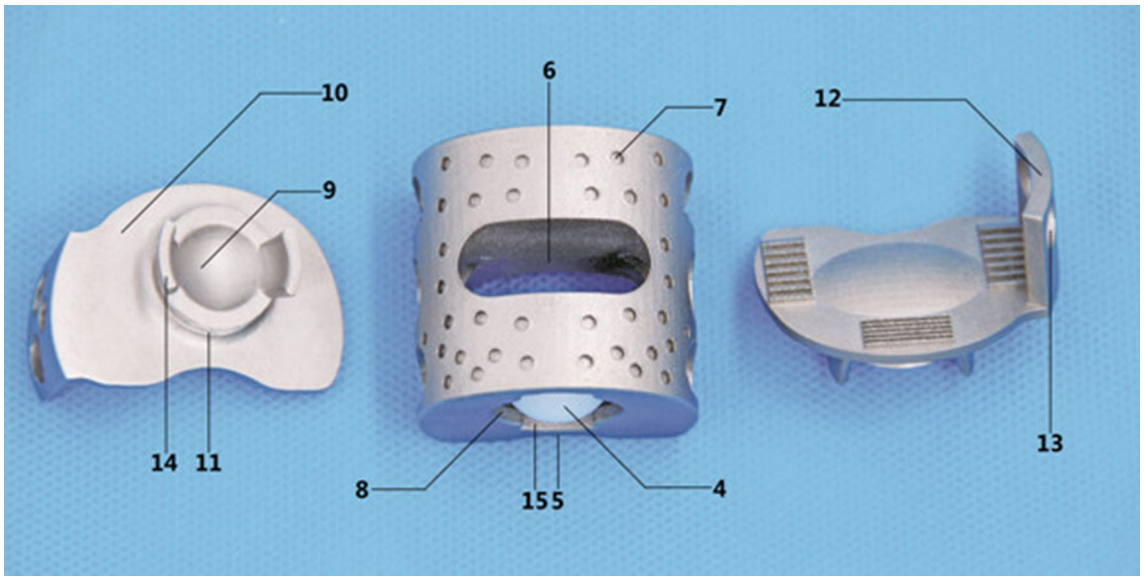

Fig. 3 Photograph of the MALC prosthesis. The number refers to the same structure as that in Fig. 2

to keep the specimens in a set position with the L3 vertebra parallel to the horizontal plane.

To evaluate the stability and movement of the prosthesis, we tested six ROM movements under a load of a maximum of 7.5 N m of torque according to the literature [19–21]: flexion (FLX), extension (EXT), right lateral bending (RLB), left lateral bending (LLB), right rotation (RR) and left rotation(LR). Because the MTS 858 Mini Bionix II machine in our laboratory cannot bend a specimen directly, we designed a new fixture (Fig. 4a) that allows the specimens to move to one side. Then, the pressure administered from the loading handle on the MTS 858 Mini Bionix II machine could be conducted through the fixture to slightly push and bend the specimen. The distance between the bottom center of the specimen and the loading handle was fixed at 5 cm. However, the machine can rotate the specimens indirectly so that we can place a specimen in the center of the loading handle of the machine and apply the pressure (Fig. 4b). We set up the MTS 858 Mini Bionix II system to provide a constant load (0.01 N m/1 s), and the axial force, axial displacement or torsion angle was recorded once every second. Because the machine cannot directly provide the bending angles, we attached some markers for the T12, L1, L2 and L3 vertebral segments, and their locations were recorded by two cameras from two fixed angles at zero loading pressure and the maximum loading pressure (7.5 N m torque). Then, the markers in the images were identified using a computer image processing system, and the movement angles between segments were calculated as the ROM. Torsion ROM between the segments was not measured due

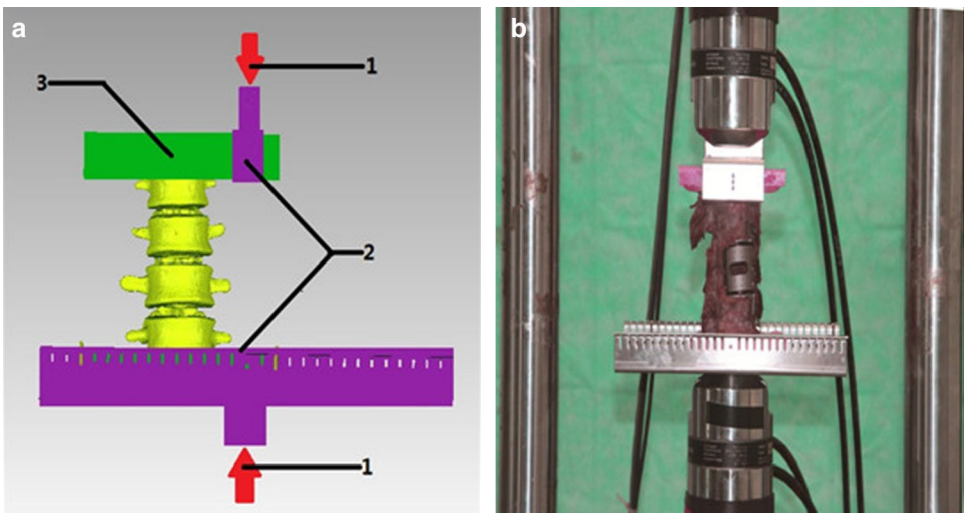

Fig. 4 Images of biomechanical tests. **a** Pattern graph of left lateral bending: 1 The location of the pressure applied, 2 The new fixture that we designed, 3 The PMMA embedding material; **b** Images of the non-fusion group in the torsion test

to technical limitations. To allow preconditioning of the specimens and to minimize the viscoelastic effect, each pressure was loaded and released three times, but only the third load cycle was evaluated and used for further analysis. During the test, saline was used every five minutes to keep each specimen moist.

Regarding the evaluation of load-bearing strength of the MALC prosthesis, we applied vertical pressure to specimens containing prostheses following ROM measurements. The loading handle of the MTS 858 Mini Bionix II machine pressed the specimens at a speed of 0.5 mm/s until significant vertebral fracture or prosthetic deformation was seen by the eye, and the axial displacement and load were recorded once every second. Then, load–displacement graphs were drawn using GraphPad Prism 5 (Version 5, GraphPad Software, Inc.), and the detailed load values were determined when a vertebra fractured or the prosthesis became deformed, according to the variation in the curve in the graph.

Statistical analysis

The data were analyzed using SPSS software (Version 21, International Business Machines Corp., USA). The results are presented as the means ± SD. The ROMs were analyzed using one-way ANOVA to directly generate the F and P values among the groups. Pairwise comparisons were conducted using the LSD test if $P > 0.05$ in the homogeneity test of variances (VHT); otherwise, the Tamhane test was used. The load-bearing strength was analyzed using two-tailed independent sample t tests. P values less than 0.05 were considered significant.

Results

Specimen selection

All the specimens included in the study had no fractures, deformity or osteoporosis. The bone mineral density (BMD) of specimens in different groups was not significantly different ($P > 0.05$), and the data are shown in Table 1.

Postoperative imaging assessment

The imaging results, including X-ray images and 3D-CT, are shown in Fig. 5a–f. According to these results, the implants were in the appropriate positions with no prosthesis dislocation, screw penetrations into the spinal canal in either of the groups. Additionally, the height of the vertebra was reconstructed using the MALC implants, and the artificial discs

Table 1 Average BMD (bone mineral density) of vertebral bodies from T12 to L3 in the three groups (g/cm^2)

Group	Number of specimens	T12	L1	L2	L3	Average
Intact group	5	0.998	1.010	1.092	1.412	1.060
fusion group	5	0.932	0.992	1.053	1.100	1.020
Non-fusion group	5	1.043	0.951	0.972	0.973	0.985

There were no significant differences in BMD of vertebral bodies from T12 to L3 among the three groups ($P > 0.05$)

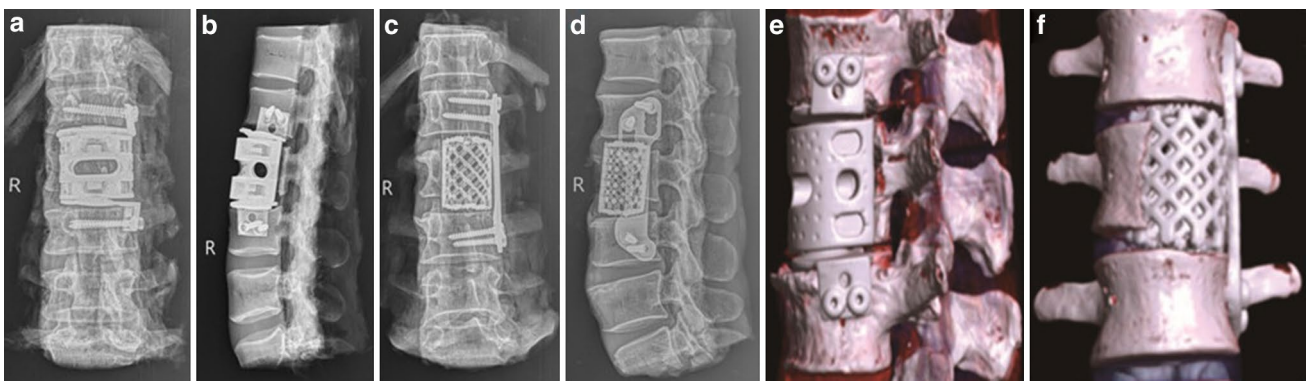

Fig. 5 Photographs of the postoperative imagiological examinations. **a, b** Anterior–posterior and lateral X-ray images of a non-fused specimen; **c, d** anterior–posterior and lateral X-ray images of a fused specimen; **e** three-dimensional reconstruction of a non-fused specimen; **f** three-dimensional reconstruction of a fused specimen

were firmly attached to the adjacent vertebrae. Spinal cord compression was not observed.

Test of stability and mobility

The range of motion (ROMs) of the surgical area and adjacent inter-vertebral discs in flexion/extension, lateral bending and axial rotation in all groups are shown in Table 2. Compared with the intact group, the non-fusion group showed no significant difference in the ROM of the T12–L1 disc in flexion/extension and lateral bending ($P > 0.05$), while the ROM of the T12-L1 disc in the fusion group showed a significant increase in the above orientations ($P < 0.05$; Fig. 6). Compared with the intact and non-fusion groups, the fusion group showed significantly smaller ROMs of L1–2 and L2–3 discs in flexion, extension and left/right lateral bending ($P < 0.05$), but the difference in ROM was not significant for L1–2 or L2–3 in the above orientations between the non-fusion and intact groups ($P > 0.05$; Fig. 7). The T12–L3 ROM in axial rotation of the non-fusion group was larger than that of the intact group and the fusion group but no significant difference existed ($P > 0.05$). Though T12–L3 ROM in the axial rotation of the fusion group was smaller than that of the intact group, significant difference was not observed ($P > 0.05$).

Evaluation of load bearing strength

The change in the trend of the axial compression force with increasing displacement is shown in Fig. 8. The first turning

Table 2 Average ROM of the specimens in the intact, fusion and non-fusion groups in response to the maximum load of 7.5 N m and comparisons between each other (in degrees)

Item	ROM_{intact} (mean ± SD)	ROM_{fusion} (mean ± SD)	$ROM_{non\text{-}fusion}$ (mean ± SD)	F	P	P_{VHT}	$P_{fusion,\ intact}$	$P_{fusion,\ non\text{-}fusion}$	$P_{intact,\ non\text{-}fusion}$
FLX_{T12-L1}	3.98 ± 0.90	5.28 ± 0.83	3.68 ± 0.86	4.831	0.029	0.820	0.035	0.013	0.594
EXT_{T12-L1}	3.74 ± 0.91	5.32 ± 0.42	3.52 ± 0.86	8.278	0.006	0.025	0.041	0.018	0.974
LLB_{T12-L1}	2.94 ± 1.10	4.72 ± 1.10	2.64 ± 0.93	5.758	0.018	0.859	0.020	0.009	0.659
RLB_{T12-L1}	2.96 ± 0.86	4.94 ± 1.17	2.58 ± 0.76	8.944	0.004	0.587	0.006	0.002	0.538
FLX_{L1-2}	4.10 ± 0.53	1.10 ± 0.35	4.62 ± 0.51	81.187	< 0.001	0.895	< 0.001	< 0.001	0.107
EXT_{L1-2}	3.72 ± 0.42	1.28 ± 0.31	4.34 ± 0.67	54.748	< 0.001	0.927	< 0.001	< 0.001	0.068
LLB_{L1-2}	2.74 ± 0.50	0.84 ± 0.34	3.16 ± 0.55	34.263	< 0.001	0.352	< 0.001	< 0.001	0.185
RLB_{L1-2}	3.04 ± 0.40	0.80 ± 0.43	3.28 ± 0.41	54.493	< 0.001	0.150	< 0.001	< 0.001	0.378
FLX_{L2-3}	4.26 ± 0.72	1.14 ± 0.30	4.54 ± 0.58	56.903	< 0.001	0.433	< 0.001	< 0.001	0.444
EXT_{L2-3}	4.08 ± 0.77	1.18 ± 0.28	4.36 ± 0.65	42.978	< 0.001	0.261	< 0.001	< 0.001	0.475
LLB_{L2-3}	3.00 ± 0.36	0.94 ± 0.36	3.26 ± 0.21	79.196	< 0.001	0.607	< 0.001	< 0.001	0.222
RLB_{L2-3}	3.20 ± 0.31	1.06 ± 0.32	3.42 ± 0.37	76.101	< 0.001	0.838	< 0.001	< 0.001	0.318
LR_{T12-L3}	4.47 ± 0.99	3.85 ± 0.50	4.60 ± 0.90	1.176	0.342	0.565	0.255	0.178	0.820
RR_{T12-L3}	4.40 ± 0.70	3.72 ± 0.70	4.50 ± 0.77	1.732	0.218	0.924	0.162	0.113	0.830

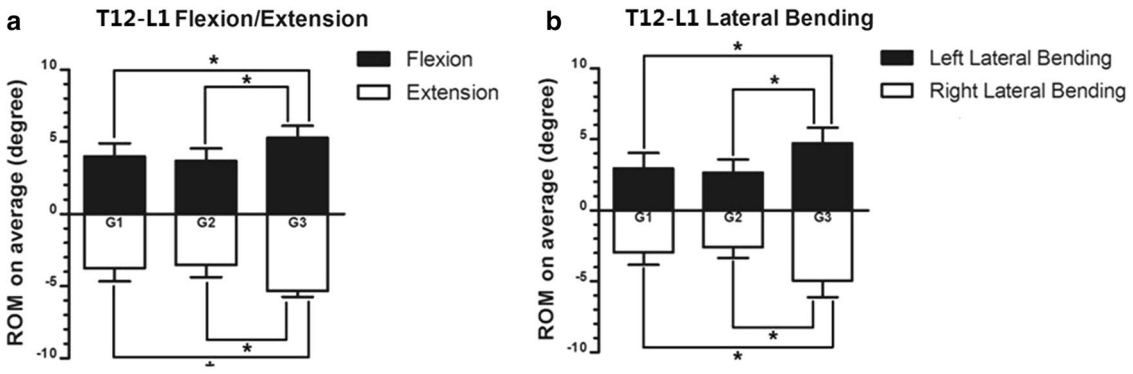

Fig. 6 T12-L1 inter-vertebral ROM under 7.5 N m of torque (loading pressure); G1-Intact group, G2-Non-fusion group, and G3-Fusion group. **a** Flexion and extension ROM, **b** left/right lateral bending ROM. The ROM in the fusion group was higher than that in the other two groups with respect to FLX, ETX, LLB and RLB; *Represents $P < 0.05$

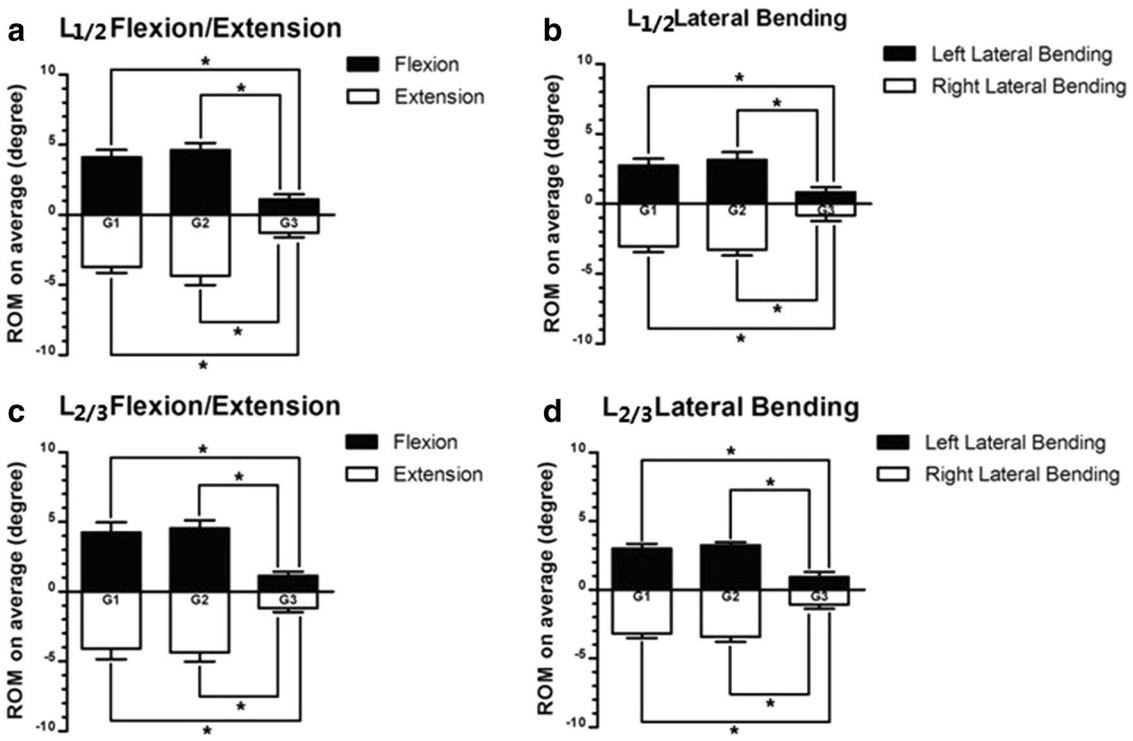

Fig. 7 L1–2/L2-3 inter-vertebral ROM under 7.5 N m of torque (loading pressure) in the G1-Intact group, G2-Non-fusion group, and G3-Fusion group. **a** L1–2 flexion and extension ROM; **b** L1–2 left lateral and right lateral bending ROM; **c** L2–3 flexion and extension ROM; **d** L2–3 left lateral and right lateral bending ROM. The ROM of L1–2 or L2–3 in the fusion group was smaller than that in the other two groups with respect to FLX, ETX, LLB and RLB; $*P < 0.05$

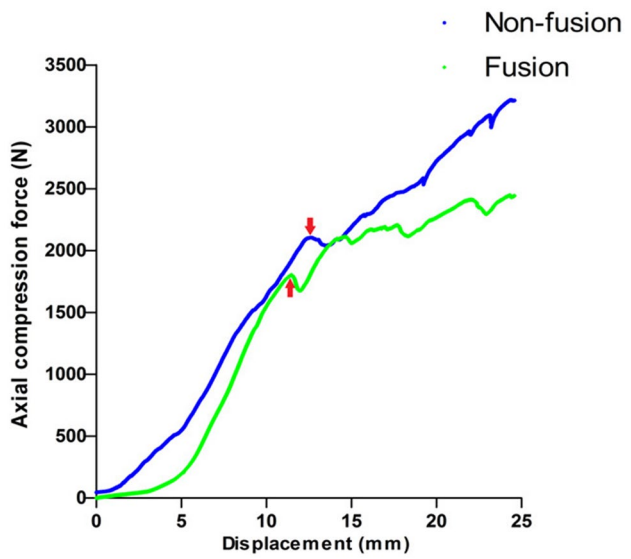

Fig. 8 Representative load–displacement curve for the MALC and titanium mesh prostheses. The red arrow represents the first turning point in the curve

point in the curve generally indicates a vertebral fracture. Although the load pressure in the non-fusion group was greater than that in the fusion group when the vertebrae of the specimens were fractured (non-fusion group versus Fusion group = 2146 ± 132 N VS 1943 ± 160 N), no significant difference was observed ($P = 0.061$). Additionally, none of the prostheses were damaged when the vertebrae of all the specimens in the fusion and non-fusion groups showed significant compression fractures.

Discussion

Vertebral corpectomy combined with interbody fusion has become a common treatment for lumbar tumor, fracture, kyphosis and other diseases [7]. The procedure involves the fusion of three or more lumbar vertebrae and removal of the disc; consequently, the dynamic function of the fused segment is considerably changed, which can increase pressure within the adjacent discs and facet joints, accelerating the degeneration of adjacent inter-vertebral discs [10]. Therefore, preserving the physiological motor function of the spine on the premise of reconstructing the stability of the spine may be the future development direction of implants. Although a variety of artificial vertebral bodies were developed in recent years and have achieved good results in the reconstruction of spine sequence and stability [22–25], few prostheses can preserve the ROM of the surgical area.

Artificial lumbar discs and other movable implants are limited by their inability to replace the resected vertebral bodies and reconstruct the vertebral height. Thus, a novel prosthesis based on the advantages of artificial vertebrae and artificial inter-vertebral discs was urgently needed in clinics. Some previously described [26–28] novel prostheses that were designed for the cervical spine and yielded good results from animal experiments have been reported. However, these prostheses cannot be directly used in the lumbar spine because of the substantial differences in physiological function and surgical approach between the cervical and lumbar spine. Consequently, we specifically designed the movable prosthesis for the lumbar spine.

According to the literature and Chinese patent review, some motion-preserving prostheses for the lumbar spine have been developed. However, all these prostheses have some defects that cannot be ignored, such as bone graft difficulty, poor mobility, and the centers of rotation of these prostheses not lying within the inter-vertebral space. Thus, we designed a new MALC that contained three parts, namely, two discs and a vertebra. The articular surface of the ball-and-socket joint of this prosthesis, which is designed similarly to an artificial knee joint, is metal on polyethylene to avoid the noise and debris associated with metal friction. The curved convex structure resists dislodgement and may maintain the stability of the ball-and-socket joint and avoid the dislocation of the implant. To achieve the instant stability of the prosthesis, we fixed the base part of the artificial disc of the MALC to the end plate of the adjacent vertebra with two screws that were not in the same horizontal plane, and we used a hydroxyapatite (HA) layer and bone grafting slots to fuse the prosthesis with surrounding residual bone to achieve long-term stabilization. To reduce the high rate of subsidence reported with the use of titanium mesh [29], we deliberately increased the contact area of the artificial disc with the end plate.

The MALC implants were in the appropriate positions in all cases, and no prosthesis dislocation, screw penetration into the spinal canal were observed in the non-fusion group, which suggested that the prosthesis reconstructed the vertebral height effectively. Regarding the stability of the prosthesis, the non-fusion group showed no significant difference in the ROM of the T12–L1, L1–2 and L2–3 inter-vertebral discs in flexion/extension and lateral bending ($P > 0.05$), suggesting a satisfactory instant stabilization. Theoretically, the MALC prosthesis decreased the ROM of the adjacent levels due to the preservation of the ROM at the surgical site. As expected, the T12–L1 flexion/extension and lateral bending ROM in the non-fusion group was smaller than that in the fusion groups, while the L1–2 and L2–3 flexion/extension and lateral bending ROM was larger than that in the fusion groups ($P < 0.05$). Although T12–L1 ROM in the non-fusion group was less than that in the intact group, this difference was not significant ($P > 0.05$). Thus, we believe that the MALC prosthesis has the potential to not only reduce the force on adjacent discs but also preserve the physiological function of the adjacent segments to some extent. In terms of rotation ROM, the non-fusion group was larger than the intact and fusion groups, but no significant difference existed ($P > 0.05$). Though the rotation ROM in the fusion group was smaller than that in the intact group, but no significant differences were observed, too ($P > 0.05$). The possible reasons were as follows: first, the MALC prosthesis allowed 360° of axial rotation, which inevitably led to an increase in rotational ROM postoperatively, which needs to be improved in the future; second, the test was performed in a cadaver, with no surrounding muscle protection, leading to increased movement; and third, the prosthesis had not been fused with the surrounding bone, and the anti-torsion power of the titanium plates was weaker. Theoretically, the MALC prosthesis preserves the ROM of the disc, which was 5° in flexion, extension, and lateral bending. However, in this study, we found that none of the inter-vertebral discs in the non-fusion groups had reached 5° in those directions. The possible reason was that the surrounding soft tissue affected the motion.

Regarding the evaluation of load-bearing strength, the results suggested that both the MALC and titanium mesh cage prostheses can provide the necessary strength, ductility, and toughness required for load-bearing. Although the maximum load in the non-fusion group was not significantly different from that in the fusion group ($P > 0.05$), the former was larger. This result indicates that compared with the titanium cages, the design of the base of the artificial disc of the MALC prosthesis reduces the local stress load of the adjacent vertebral endplates. Teng Lu and co-workers once studied the effects of titanium mesh cage end structures on the compressive load at the endplate interface and concluded that both the ring shape and the oblique angle of the titanium cage contributed to the increase in compressive force [30]. Thus, the base of the artificial disc designed by our teams took into full consideration the above conclusions.

The limitations of this study must be acknowledged. First, although our results suggest that the MALC prosthesis preserves the dynamic function of the inter-vertebral space and reconstructs the vertebral height, the results should be cautiously interpreted because of the study's low power. The use of a larger sample set should be considered in future studies. Second, the experiment only assessed the mechanical properties in vitro; the in vivo bio-safety and ROM, biomechanical tests with cyclic loading need further study.

It needs to be stated that the stability of the new type of prosthesis for the reconstruction of the surgical site is based on the integrity of the posterior column of the spine, so the new type of prosthesis is only applicable to patients with complete posterior column of the vertebra, such as

simple AO A1-A3 compressive fracture, benign tumors of the anterior column of the vertebra, mandatory spondylitis, etc. For spinal fractures involving the posterior column, the prosthesis is not currently available. In addition, for patients with spinal malignancy, surgery generally requires total vertebral resection, and patients generally have a short survival period, the new prosthesis cannot be used. For patients with spinal infection, we always believe that the stability of the reconstructive surgical site is the most important, and whether the implantation of movable prosthesis will cause infection recurrence, prosthesis displacement and other complications still need further experimental study. However, vertebrae resection and fusion has been applied in the field of spine for decades, and it is becoming increasingly perfect in the realization of spinal cord decompression and reconstruction of spinal stability. Therefore, how to restore the motor function of the spine on the basis of ensuring the above operation results may become a new research direction of spinal surgery in the twenty-first century. Although the limited indications for the new prosthesis and the need for further improvement in its construction, it is believed that with the continuous development of science and technology, the transformation of the concept of spinal surgery treatment and the continuous improvement of the design of the new prosthesis, its indications may also continue to increase, and it is likely to occupy a place in clinical practice.

In conclusion, biomechanical testing was performed in vitro in this study to assess the MALC prosthesis. Compared with lumbar interbody fusion, the use of a MALC prosthesis not only restored vertebral height but also effectively preserved segment movements in flexion/extension and lateral bending, without any abnormal gain of mobility in adjacent inter-vertebral spaces. The MALC prosthesis also demonstrated appropriate lumbar load-bearing and reduced the local stress load of adjacent vertebral endplates. However, the defect in axial rotation angle should be further improved, and in vivo animal experiments and other studies will be necessary to evaluate the biocompatibility and tribological properties of this movable prosthesis.

Acknowledgements I would like to express my gratitude to Lu Teng and Liang Hui. They gave us a lot of support and help during the study. I also owe a special debt of gratitude to the fund "The 2016th Science and technology breakthrough project of Henan province" (No. 162102310018) and "Henan provincial science and technology innovation outstanding talent project" (154200510027). In the financial support of them, we finally successfully completed this experiment.

References

1. Chen B et al (2015) Comparison of the therapeutic efficacy of surgery with or without adjuvant radiotherapy versus radiotherapy alone for metastatic spinal cord compression: a meta-analysis. World Neurosurg 83(6):1066–1073
2. Wang H et al (2012) Epidemiology of spinal fractures among the elderly in Chongqing, China. Inj Int J Care Inj 43(12):2109–2116
3. Bradford R et al (2017) Anterior lumbar corpectomy with expandable titanium cage reconstruction—a case series of 42 patients. World Neurosurg 108:317–324
4. Kang C-N et al (2013) Anterior operation for unstable thoracolumbar and lumbar burst fractures tricortical autogenous iliac bone versus titanium mesh cage. J Spinal Disord Tech 26(7):E265–E271
5. Pingel A, Castein J, Kandziora F (2017) Anterior monosegmental stabilization and fusion of an incomplete cranial burst fracture in the thoracolumbar spine via a mini-open, thoracoscopically assisted transthoracic approach. Eur Spine J 26:431–432
6. Scholz M et al. (2017) Prospective randomized controlled comparison of posterior vs. posterior–anterior stabilization of thoracolumbar incomplete cranial burst fractures in neurological intact patients: the RASPUTHINE pilot study. Eur Spine J 27:3016–3024
7. Liu P et al (2015) A retrospective controlled study of three different operative approaches for the treatment of thoracic and lumbar spinal tuberculosis: three years of follow-up. Clin Neurol Neurosurg 128:25–34
8. Zhang C et al (2016) Adjacent segment degeneration versus disease after lumbar spine fusion for degenerative pathology a systematic review with meta-analysis of the literature. Clin Spine Surg 29(1):21–29
9. Pan A et al (2016) Adjacent segment degeneration after lumbar spinal fusion compared with motion-preservation procedures: a meta-analysis. Eur Spine J 25(5):1522–1532
10. Kim H-J et al (2015) The influence of intrinsic disc degeneration of the adjacent segments on its stress distribution after one-level lumbar fusion. Eur Spine J 24(4):827–837
11. Lu S-b et al (2015) An 11-year minimum follow-up of the Charite III lumbar disc replacement for the treatment of symptomatic degenerative disc disease. Eur Spine J 24(9):2056–2064
12. Wuertinger C et al (2017) Motion preservation following total lumbar disc replacement at the lumbosacral junction: a prospective long-term clinical and radiographic investigation. Spine J 18:72–80
13. Ma Y-Z et al (2008) The mid- or long-term clinical results of prosthetic disc nucleus replacement in the treatment of lumbar disc disease. Zhonghua wai ke za zhi [Chinese journal of surgery] 46(5):350–353
14. Kashkoush A et al (2016) Evaluation of a hybrid dynamic stabilization and fusion system in the lumbar spine: a 10 year experience. Cureus 8(6):e637–e637
15. Liu J et al (2017) Lumbar subtotal corpectomy non-fusion model produced using a novel prosthesis. Arch Orthop Trauma Surg 137(11):1467–1476
16. Liu J, Li H, Niu B (2017) Design and activity analysis of bionic artificial lumbar vertebra and disc complex. Orthop Biomech Mater Clin Stud 14(2):5–10
17. Lu T et al (2017) Single-level anterior cervical corpectomy and fusion using a new 3D-printed anatomy-adaptive titanium mesh cage for treatment of cervical spondylotic myelopathy and ossification of the posterior longitudinal ligament: a retrospective case series study. Med Sci Monit 23:3105–3114
18. Wilke HJ, Wenger K, Claes L (1998) Testing criteria for spinal implants: recommendations for the standardization of in vitro stability testing of spinal implants. Eur Spine J 7(2):148–154
19. Disch AC et al (2007) Three-dimensional stiffness in a thoracolumbar en-bloc spondylectomy model: a biomechanical in vitro study. Clin Biomech 22(9):957–964
20. Disch AC et al (2008) En bloc spondylectomy reconstructions in a biomechanical in-vitro study. Eur Spine J 17(5):715–725

21. Wilke HJ, Kettler A, Claes LE (1997) Are sheep spines a valid biomechanical model for human spines? Spine 22(20):2365–2374
22. Ramirez JJ et al (2010) An expandable prosthesis with dual cage-and-plate function in a single device for vertebral body replacement: clinical experience on 14 cases with vertebral tumors. Arch Med Res 41(6):478–482
23. Khodadadyan-Klostermann C et al (2004) Expandable cages: biomechanical comparison of different cages for ventral spondylodesis in the thoracolumbar spine. Chirurg 75(7):694–701
24. Penzkofer R et al (2011) Biomechanical comparison of the end plate design of three vertebral body replacement systems. Arch Orthop Trauma Surg 131(9):1253–1259
25. Vieweg U (2007) Vertebral body replacement system Synex in unstable burst fractures of the thoracic and lumbar spine. J Orthop Traumatol 8(2):64–70
26. Qin J et al (2012) Artificial cervical vertebra and intervertebral complex replacement through the anterior approach in animal model: a biomechanical and in vivo evaluation of a successful goat model. PLoS One 7(12):e52910
27. Dong J et al (2015) Artificial disc and vertebra system: a novel motion preservation device for cervical spinal disease after vertebral corpectomy. Clinics 70(7):493–499
28. Yu J, Liu L-T, Zhao J-N (2013) Design and preliminary biomechanical analysis of artificial cervical joint complex (vol 133, pg 735, 2013). Arch Orthop Trauma Surg 133(9):1329–1329
29. Jang J-W et al (2014) Effect of posterior subsidence on cervical alignment after anterior cervical corpectomy and reconstruction using titanium mesh cages in degenerative cervical disease. J Clin Neurosci 21(10):1779–1785
30. Lu T et al (2017) Effects of titanium mesh cage end structures on the compressive load at the endplate interface: a cadaveric biomechanical study. Med Sci Monit 23:2863–2870